Infrared optical absorption in imperfect parabolic quantum wells

L. Brey, Jed Dempsey, N. F. Johnson, and B. I. Halperin
Lyman Laboratory of Physics, Harvard University, Cambridge, Massachusetts 02138
(Received 26 February 1990)

The effects of possible imperfections on the infrared optical absorption and on the charge-density profile of wide parabolic quantum wells (WPQW's) are studied. We consider effects that can arise from the finite width of WPQW's, from the existence of a quartic component in the confining potential, and from the existence of a region of flat potential in the center of the well. Within the local-density approximation, we confirm that a perfect WPQW absorbs light only at the bare harmonic-oscillator frequency, and show that the effects of small imperfections of the types considered on the absorption spectrum are twofold: a shift in the location of the main peak and the appearance of new peaks nearby.

I. INTRODUCTION

The properties of an interacting three-dimensional (3D) electron gas in a uniform positive background have been widely studied over the years[1] and different many-body effects have been predicted. In particular, the ground state of this system in an external magnetic field is expected to be a spin-density wave or a Wigner crystal when the electron density is low enough.[2] In order to observe these broken-symmetry ground states, a lower density of electrons than that found in normal metals is required. For this reason, n-type doped semiconductors with small effective mass and low carrier density might seem the best candidates to exhibit exotic ground states. Unfortunately, the interaction between the electrons and the neutralizing charged impurities in these systems is strong enough[3] to preclude any broken-symmetry ground state favored by the electron-electron interaction. In contrast, the study of a high-mobility, two-dimensional (2D) electron gas has been possible experimentally,[4] due in part to the development of modulation-doping techniques, which reduce the electron-ionized impurity interaction by separating the 2D electron gas spatially from the neutralizing positive charges.

To achieve an almost-3D electron gas while reducing the electron-impurity interaction, a remotely doped wide–parabolic-quantum-well (WPQW) structure has been proposed.[2] In such a well, the parabolic potential, $V(z)=Az^2$, mimics the potential created by a uniform slab of positive charge of density $n_0=A\epsilon/2\pi e^2$. In this expression, e is the electron charge and ϵ is the (uniform) static dielectric constant of the host semiconductor. Electrons are introduced remotely in the WPQW by placing donors at some distance from either side of the well. The electrons enter the well to screen the parabolic potential and distribute themselves in a uniform layer of density n_0 over the fictitious positive charge. In practice, the WPQW's are $\sim$4000 Å wide, and uniform electron layers of thickness $>$2000 Å have been obtained. Because the donors can be separated by several hundred angstroms from the electrons in such a system, the electron-random impurity potential can be considerably smaller than is possible in the usual doped semiconductors. The mobility of these samples, even in the presence of alloy-disorder scattering, should be significantly higher than that of doped semiconductors with the same concentration of carriers.

In the experimental samples, the parabolic potential is achieved by tailoring the conduction-band edge of an alloy semiconductor, usually $Ga_{1-x}Al_xAs$. Since the band offset between GaAs and $Ga_{1-x}Al_xAs$ is proportional[5] to x, it is possible to obtain a parabolic potential by varying the fraction of aluminum quadratically with position. Recently, structures of this type were grown using molecular-beam epitaxy by Gossard and co-workers,[6] and independently by Shayegan and co-workers.[7] Magneto-transport experiments[6,7] on these WPQW's reveal that they hold a thick, high-mobility slab of electron gas. In addition, recent theoretical studies of these systems have discussed electron energy levels and charge-density profiles,[8] electronic structure in the presence of a longitudinal magnetic field,[9] and the existence of a spin-density-wave instability in the presence of a longitudinal magnetic field.[10]

The infrared optical absorption and magneto-optical absorption in WPQW have been studied experimentally[11] and theoretically.[12] It has been shown[12] that, in the absence of an applied magnetic field, an ideal n-type doped parabolic quantum well absorbs far-infrared radiation only at the bare harmonic oscillator frequency, independent of the electron-electron interaction and of the number of electrons in the well. For this reason, it has been thought that optical-absorption measurements might be useful in characterizing departures from ideal parabolicity in experimental samples.

The aim of the present work is to study, within the framework of the Hohenberg-Kohn-Sham local-density approximation (LDA), how the optical absorption of a WPQW changes from its ideal form when different imperfections are present. We also report the influence of imperfections on the charge-density profile and on the electronic states. In Sec. II we describe the method used

in our calculations, and in Sec. III we discuss three experimentally relevant[6] effects: the effect of the finite width of the well, the effect of a quartic term added to the parabolic potential, and the effect of a region of flat potential in the center of the well. Finally, in Sec. IV, we summarize our results.

In the present paper we confine ourselves to the case of zero applied magnetic field. If one can neglect the scattering of electrons by impurities and phonons, the absorption in this case is produced only by the component of the electric field in the z direction (perpendicular to the layer). Thus, to see the effect, one must use radiation that is incident at an angle far from normal incidence.

II. METHOD OF CALCULATION

We consider a WPQW with the geometry used in Ref. 6, where the well has a finite width W, a depth Δ_1, and is bounded by an additional barrier of height Δ_2. To describe the electrons in the host semiconductor, we use the effective-mass approximation. We take the static dielectric constant and the effective mass to be uniform across the well. In the actual WPQW,[6,7] these quantities vary by only 11 and 7%, respectively, from the center to the edge of the well, and including this variation in the calculation produces only small changes in the results. Also omitted from the calculation are the nonparabolicity of the conduction band and the band-mixing effects induced by confinement. These effects, again, have only a small influence on the electronic properties of the system.

The interactions between electrons in the conduction band can be separated into a Hartree term due to the electrostatic potential of the total electron density and an exchange-correlation term.[1] The exchange-correlation part of the ground-state energy can be described as a functional of the electron density.[13] In the LDA this functional is assumed to have only local dependence on the electron density. The LDA has been used very successfully to obtain ground-state properties of many systems.[14] Making this local approximation leads to a one-body Schrödinger-type equation, where the electrons move in a potential that is the sum of the external (parabolic) potential, the Hartree potential, and an exchange-correlation potential. Although the energy eigenvalues of this one-particle equation do not correspond to the quasiparticle energies, one can consider the exchange-correlation potential as a local, energy-independent self-energy.[15] The LDA gives good results for conduction electrons in silicon inversion layers and $GaAs/Ga_{1-x}Al_xAs$ heterostructures, and for quantum wells.[4,16]

In our system, we replace the localized donor charges by a z-dependent charge density that has been averaged over the x-y plane. If we restrict ourselves to self-consistent solutions that respect translational symmetry in the x-y plane, the one-electron equation describing the motion of the electrons separates, and the wave functions and eigenvalues are

$$E_{n,k_x,k_y}=\varepsilon_n+\frac{\hbar^2k_x^2}{2m^*}+\frac{\hbar^2k_y^2}{2m^*}\ , \tag{1a}$$

$$\Psi_{n,k_x,k_y}(\mathbf{r})=\frac{1}{\sqrt{S}}e^{i(k_xx+k_yy)}\varphi_n(z)\ , \tag{1b}$$

where we have supposed spin degeneracy and omitted the spin index. In the above expression, S is the sample area, $\mathbf{k}=(k_x,k_y)$ is the wave vector of the electron, m^* is the effective mass, and ε_n and $\varphi_n(z)$ are obtained from the one-dimensional Schrödinger equation

$$\left[-\frac{\hbar^2}{2m^*}\frac{d^2}{dz^2}+V(z)+V_H(z)+V_{\rm xc}(z)\right]\varphi_n(z)=\varepsilon_n\varphi_n(z)\ . \tag{2}$$

In this expression, $V(z)$ is the bare well potential, which depends on the Al concentration at the position z, and which corresponds to the position of the bottom of the conduction band in the absence of doping; $V_{\rm xc}(z)$ is the exchange-correlation potential[17]

$$V_{\rm xc}(z)=-0.985\frac{e^2}{\epsilon}n^{1/3}(z)\left[1+\frac{0.034}{a_B^*n^{1/3}(z)}\ln[1+18.376a_B^*n^{1/3}(z)]\right]\ , \tag{3}$$

where $a_B^*=\epsilon\hbar^2/m^*e^2$; $V_H(z)$ is the Hartree term due to the electrostatic interaction of the electrons with themselves and with the [(x,y)-averaged] impurity charge,

$$\frac{d^2V_H(z)}{dz^2}=-\frac{4\pi e^2}{\epsilon}[n(z)-N_D(z)]\ , \tag{4}$$

where $N_D(z)$ is the density of positive charge necessary to maintain charge neutrality. The electron density $n(z)$ is given by

$$n(z)=\sum_i n_i(z)\ ,$$
$$n_i(z)=\frac{m^*}{\pi\hbar^2}(\varepsilon_F-\varepsilon_i)|\varphi_i(z)|^2\Theta(\varepsilon_F-\varepsilon_i)\ , \tag{5}$$

where $n_i(z)$ is the contribution of the ith subband to the charge density, $\Theta(\varepsilon)$ is the Heaviside unit-step function ($\Theta=0$ for $\varepsilon<0$ and $\Theta=1$ for $\varepsilon>0$), and ε_F is the Fermi energy obtained from the condition

$$n_s=\sum_i N_i\ ,$$
$$N_i=\frac{m^*}{\pi\hbar^2}(\varepsilon_F-\varepsilon_i)\Theta(\varepsilon_F-\varepsilon_i)\ , \tag{6}$$

N_i being the number of electrons per unit area in the ith subband. Consistent with our use of a dielectric constant that is uniform across the well, we have neglected the effect of image potentials in Eq. (2).

The self-consistent solution of Eqs. (2)–(6) gives us the charge-density profile, the Fermi energy, the subband energies, and the total potential, which is defined as $V_T(z) \equiv V(z) + V_H(z) + V_{xc}(x)$. From the eigenfunctions and eigenvalues, we can obtain the infrared (ir) optical spectrum of the system.

The peaks in the ir optical absorption do not appear at frequencies corresponding to the quasiparticle energy separation. Instead, the resonances are shifted from the self-consistent subband separation by the depolarization effect,[18] due to the Hartree screening of the resonance, and by the excitoniclike[19] or vertex-correction effect. In fact, the absorption peaks correspond to the collective modes of the system, which must be determined from the poles of the appropriate response function.[20] In the case of a quantum well, in the long-wavelength limit, the movement of the confined electrons can only be coupled to an electric field perpendicular to the electronic sheet, and the charge in the well absorbs ir radiation only if the electric field has a component in the perpendicular direction. We are able to use the dipole approximation in describing the interaction between light and the electrons and to neglect retardation effects[21] because the thickness of the typical WPQW is much smaller than the wavelength of the light with frequency corresponding to the self-consistent subband separation.

We obtain the optical absorption by using the self-consistent-field approximation[22] together with the LDA. In the form derived by Ando,[19] the optical absorption per unit area can be written as

$$P(\omega) = \tfrac{1}{2}\,\mathrm{Re}[\tilde{\sigma}_{zz}(\omega) D^2] \,, \tag{7}$$

where D is the external electric field directed in the z direction and $\tilde{\sigma}_{zz}$ is the modified two-dimensional dynamical conductivity

$$\tilde{\sigma}_{zz}(\omega) = \frac{e^2}{m^*}(-i\omega) n_s \sum_l \frac{\tilde{f}_l}{\tilde{E}_l^2 - (\hbar\omega)^2 - 2i\hbar\omega/\tau} \,, \tag{8}$$

where we have introduced a phenomenological relaxation time τ and

$$\tilde{f}_l = \left[\sum_{n,n'} \left[\frac{2m^*}{\hbar^2}(\varepsilon_n - \varepsilon_{n'}) \right]^{1/2} \times Z_{n'n} \left[\frac{N_n - N_{n'}}{n_s} \right]^{1/2} U_{n'n,l} \right]^2 , \tag{9}$$

where $Z_{n'n}$ is the matrix element of the z coordinate between the states $\varphi_{n'}$ and φ_n. $\tilde{E}_l^2$ in Eq. (8) and $U_{n'n,l}$ in Eq. (9) are the eigenvalues and eigenfunctions of the matrix

$$\Lambda_{nn',mm'} = E^2_{n'n}\delta_{n'm'}\delta_{nm} + (N_n - N_{n'})^{1/2}(N_m - N_{m'})^{1/2} \times (E_{m'm}E_{n'n})^{1/2}(\alpha_{nn',mm'} - \beta_{nn',mm'}) \,. \tag{10}$$

In the above expressions, the indices n, n', m, and m' refer to the eigenvalues and eigenvectors of the one-dimensional equation (2). The matrix elements α and β in Eq. (9) represent the depolarization and excitonic effects, respectively, and are given by the expressions

$$\alpha_{nn',mm'} = -2\frac{4\pi e^2}{\epsilon} \int_{-\infty}^{+\infty} dz\, \varphi_n(z)\varphi^*_{n'}(z) \times \int_{-\infty}^{z} dz' \int_{-\infty}^{z'} dz''\, \varphi_m(z'') \times \varphi^*_{m'}(z'') \,, \tag{11}$$

$$\beta_{nn',mm'} = -2\int_{-\infty}^{+\infty} \varphi_n(z)\varphi^*_{n'}(z)\frac{\partial V_{xc}}{\partial n(z)}\varphi_m(z)\varphi^*_{m'}(z)dz \,. \tag{12}$$

It is also easy to show that the two-dimensional dynamical conductivity satisfies the sum rule

$$\int \tilde{\sigma}_{zz}(\omega)d\omega = \frac{e^2\pi}{m^*} n_s \,. \tag{13}$$

In this model the vertex corrections are given by the functional derivative of the exchange-correlation potential with respect to the density. That this correction is independent of frequency is consistent with the lack of dependence of the exchange-correlation potential on the quasiparticle energy. It is important to note that, to be consistent, the use of the exchange-correlation potential in the calculation of the excitoniclike effects must be accompanied by the inclusion of V_{xc} in the one-dimensional Schrödinger equation, and vice versa.

III. NUMERICAL RESULTS

We are interested in the electronic and optical properties of the model parabolic potential

$$V_1(z) = \frac{4\Delta_1 z^2}{W^2}\Theta(W/2 - |z|) + (\Delta_1 + \Delta_2)\Theta(|z| - W/2) \tag{14}$$

and in the effects that different perturbations, when added to this potential, have on those properties. In our calculations we use the following set of parameters: $\epsilon = 12.5$, $\Delta_1 = 150$ meV, $\Delta_2 = 75$ meV, and $m^* = 0.067$ times the free electron mass. The positively charged donor impurities are in two layers of equal charge density, 200 Å thick, located just outside the well on either side. We have checked that our results are insensitive to the precise location of the positive charges for reasonable choices of the parameters.

In some of the actual WPQW the parabolic potential is created by changing the relative thickness of alternating GaAs and $Al_{0.3}Ga_{0.7}As$ layers in a superlattice of period 20 Å, so that the average aluminum composition changes quadratically across the well.[6] Since the resulting potential is very difficult to handle numerically, we have used the averaged potential in our calculations. To check the sensitivity of our results to short-wavelength variations in the potential, we have compared the results for another fine superlattice with those for its averaged parabolic potential. The fine superlattice we considered had a period

of 20 Å, a fixed barrier thickness of 10 Å, and a barrier height which changed quadratically from one period to the next. The differences between the charge-density profiles obtained for the fine superlattice and for the averaged potential are very small. The superlattice produces an oscillation of very small amplitude in the charge-density profile, with the same period as the superlattice. There are also small differences in the charge-density distribution at the center of the well, due to the region of flat potential that the superlattice produces in the center of the well. This flat region typically corresponds to 3 or 5 periods of the fine superlattice. The effects on the energy levels and on the optical absorption are also small. The insensitivity of our results to fine structure in the potential arises because the reciprocal lattice vector corresponding to the superlattice period has an associated kinetic energy much larger than the energy spacing between the parabolic-well states in which we are interested. In summary, we have checked that the use of the averaged potential instead of the fine superlattice potential does not affect our results.

A. Size effects

In this subsection we study the effects of the finite width W and the additional confining potential Δ_2 on the properties of the system. We apply the method described in Sec. II to the potential of Eq. (14), $V(z)=V_1(z)$, and we study the variation of the properties of the system with the fractional occupation η defined by $\eta=n_s/(n_0W)$, where n_s is the number of electrons per unit area in the system. We have found, in agreement with Ref. 8, that the number of occupied subbands increases with the number of electrons in the well, that the separation in energies between occupied subbands decreases with n_s, and that the separation between the Fermi energy and the first subband occupied goes quickly to the 3D value $\varepsilon_F=\hbar^2(3\pi^2n_0)^{2/3}/2m^*$. We have also checked that the thickness of the electron slab increases linearly with the fractional occupation η. Our calculations show that a very uniform slab of electrons is formed when only two subbands are occupied.

Size effects become important when the fractional occupation is near 1 and the electrons feel the abrupt change in potential at the edge of the well. In Fig. 1 we plot the charge-density profile for $\eta=0.6$ and for $\eta=1$. In the $\eta=0.6$ case the charge is almost uniform in the occupied part of the well. The small bumps at the edges of the slab are Friedel-type oscillations, similar to those which appear at metal-vacuum interfaces.[23] As the WPQW moves toward complete filling ($\eta=1$), the electrons start to feel the nonparabolic confining potential (Δ_2), and the amplitude of the oscillations at the edge of the charge-density profile increases. For $\eta>1$, extra charge accumulates at the edges of the well, and the distribution of electrons becomes more and more like two 2D sheets.

Figure 2 shows the infrared optical absorption for different values of the fractional occupation η. When the number of electrons in the well is small enough, so that the charge does not feel the edges of the well ($\eta\leq 0.8$),

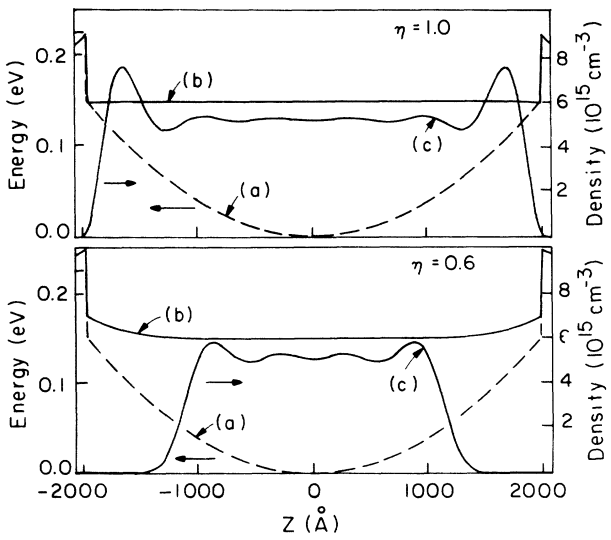

FIG. 1. Potential and charge density in a WPQW for two different fractional occupations, $\eta=0.6$ and $\eta=1$. Curve (a) shows the bare potential $V(z)$ for the well, and curve (b) shows the total self-consistent potential $V_T(z)$. Curve (c) shows the self-consistent charge-density profile $n(z)$. The parameters of the WPQW are given in the text.

the system absorbs light only at the bare frequency $\omega_0=(8\Delta_1/W^2m^*)^{1/2}$. This frequency can be identified with the plasmon frequency of a 3D electron gas of density n_0, since by construction $\omega_0=(4\pi n_0e^2/\epsilon m^*)^{1/2}$. This result is expected from the analysis of Ref. 12. In the parabolic potential there is an *exact* cancellation of the depolarization term and the vertex-correction term by

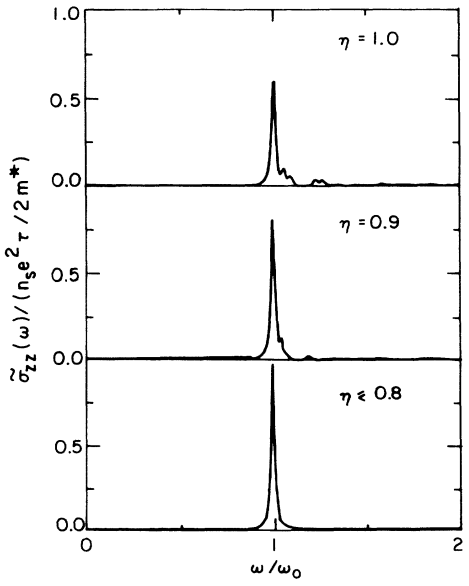

FIG. 2. Calculated real part of the dynamical conductivity $\tilde{\sigma}_{zz}(\omega)$ in a WPQW for different values of the fractional occupation η. The parameters of the WPQW are given in the text. The value of the phenomenological relaxation time, τ, is $0.01\omega_0$.

the corrections to the quasiparticle energy spacing due to the electron-electron interaction.

The effects of the finite width of the parabolic well begin to appear when $\eta \geq 0.8$. The effect of the finite width is negligible for fractional occupations smaller than 0.8 but increases quickly for higher values. For values of η smaller than 1, the perturbation is still relatively small and has two main effects on the optical absorption of the WPQW. First, the main peak in the absorption spectrum is shifted to a slightly higher frequency because the extra confinement increases the oscillation frequency of the center of mass of the electrons. Second, small satellites appear around the main peak because the electric field of the incident light can now couple to the internal motion of the electrons as well as to the motion of the center of mass.

B. Effect of a quartic term added to the parabolic potential

In this subsection we study the effect that a quartic term of the form

$$V_q(z)=\frac{16\Delta_q z^4}{W^4}\Theta(W/2-|z|) \tag{15}$$

has on the properties of the WPQW. We apply the method described in Sec. II to the potential $V(z)=V_1(z)+V_q(z)$. In order to exclude effects due to the finite width of the well, we fix the fractional occupation at $\eta=0.6$. Note that with this value of η, the ratio of the quartic potential to the parabolic potential at the edges of the electronic slab is only one-third the same ratio at the edges of the well.

In Fig. 3, we show the subband energies and the Fermi energy as a function of Δ_q. Figure 4 shows the initial potential, the self-consistent potential, and the charge-density profile for the cases $\Delta_q=-40$ and 75 meV. The behavior is quite different for different signs of Δ_q. For positive values, the quartic potential induces a convex parabolic correction to the nearly uniform charge distribution produced by the parabolic potential alone. The positive quartic potential also increases the confinement of the electrons in the well, so the subband energy spacing increases with increasing Δ_q.

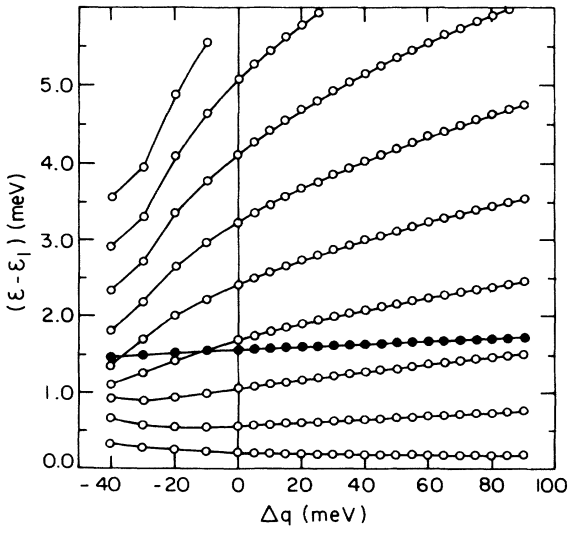

FIG. 3. Fermi level $\varepsilon_F-\varepsilon_1$ (solid circles) and energy-level separation $\varepsilon_i-\varepsilon_1$ (open circles) as a function of the strength of the quartic term Δ_q (see text). The fractional occupation η is 0.6. The parameters of the WPQW are given in the text.

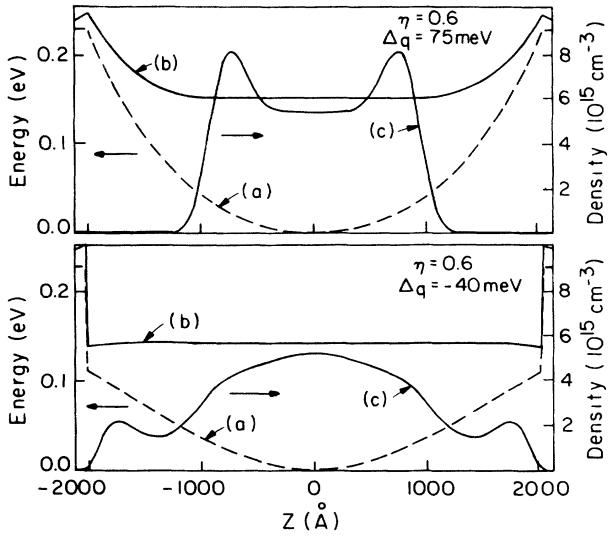

FIG. 4. Potential and charge density in a WPQW for two different values of the quartic term added to the potential: $\Delta_q=75$ meV and $\Delta_q=-40$ meV. The fractional occupation is $\eta=0.6$. Curve (a) shows the bare potential $V(z)=V_1(z)+V_q(z)$ for the well, curve (b) shows the total self-consistent potential $V_T(z)$. Curve (c) shows the self-consistent charge-density profile $n(z)$. The parameters of the WPQW are given in the text.

For negative values of Δ_q, the quartic potential adds a concave parabolic component to the charge distribution. Even a moderate negative Δ_q causes the charge to spread out considerably in the well and destroys the uniform charge-density profile. For small negative values of Δ_q, the main effect of the perturbation is to reduce the confinement of the electrons and, thus, the intersubband separation. For values of Δ_q more negative than those shown in Fig. 3, the charge builds up more and more at the edges of the well, and the energy levels approach those of two 2D electron gases.

In Fig. 5(a) we show the real part of the dynamical conductivity for different positive values of Δ_q. For small values of Δ_q the effect of the perturbation on the optical-absorption spectrum is twofold: a small shift to higher frequencies of the main peak and the appearance of small satellites around it. This is similar to the effect produced by the finite width of the well. But now instead of several peaks at higher frequencies than ω_0 there is only one additional peak. This shows that the step-potential Δ_2 allows more different transitions than the smoother quartic potential. At larger values of Δ_q the quartic term is comparable to the parabolic term and several transitions, with similar intensities, appear around ω_0.

Figure 5(b) shows the optical absorption for negative values of Δ_q. In this case, as mentioned above, moderate

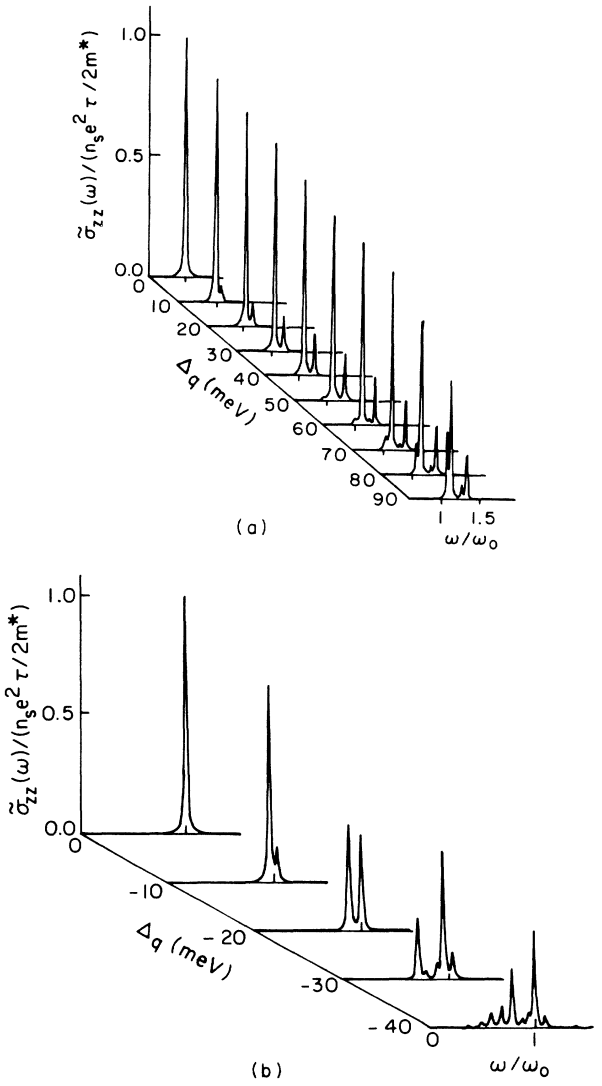

FIG. 5. Calculated real part of the dynamical conductivity $\tilde{\sigma}_{zz}(\omega)$ in a WPQW for (a) positive and (b) negative strengths of quartic term added to the potential. The fractional occupation η is 0.6. The parameters of the WPQW are given in the text. The value of the phenomenological relaxation time, τ, is $0.01\omega_0$.

values of Δ_q produce large changes in the charge-density profile, and the ir spectrum shows several peaks of comparable intensity around a main peak that is shifted down slightly from ω_0.

C. Effect of a region of flat potential in the center of the well

In this section we apply the method of Sec. II to the potential $V(z)=V_1(z)+V_{\rm fl}(z)$, where $V_{\rm fl}(z)$ is given by

$$V_{\rm fl}(z)=-\frac{4\Delta_1 z^2}{W^2}\Theta(W_{\rm fl}/2-|z|) -\frac{4\Delta_1}{W^2}\left[\frac{W_{\rm fl}}{2}\right]^2\Theta(|z|-W_{\rm fl}/2)\ . \quad (16)$$

$V_{\rm fl}(z)$ cancels $V_1(z)$ in the center of the well, producing a

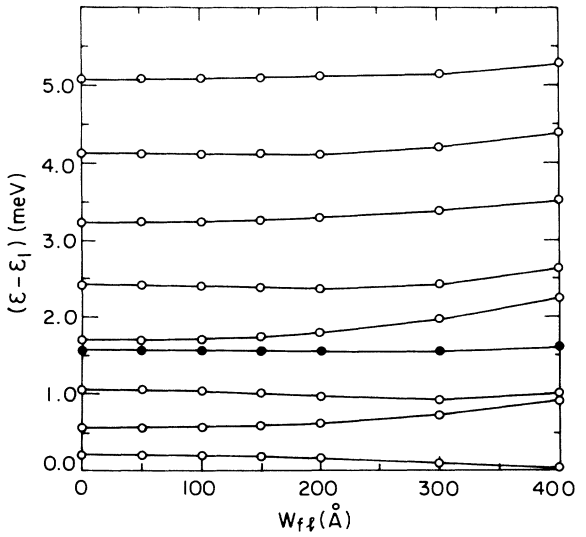

FIG. 6. Fermi level $\varepsilon_F-\varepsilon_1$ (solid circles) and energy-level separation $\varepsilon_i-\varepsilon_1$ (open circles) as a function of the width of the region of flat potential, W_{fl} (see text). The fractional occupation η is 0.6. The parameters of the WPQW are given in the text.

flat segment of potential of width $W_{\rm fl}$ centered about $z=0$. When added to the perfect parabolic potential, $V_{\rm fl}(z)$ acts as a barrier in the center of the well which tends to separate the electron gas into two 2D systems. In Fig. 6 we plot the subband energies and the Fermi energy as a function of $W_{\rm fl}$, having fixed η at 0.6 as before to eliminate finite-width effects. As $W_{\rm fl}$ increases, the

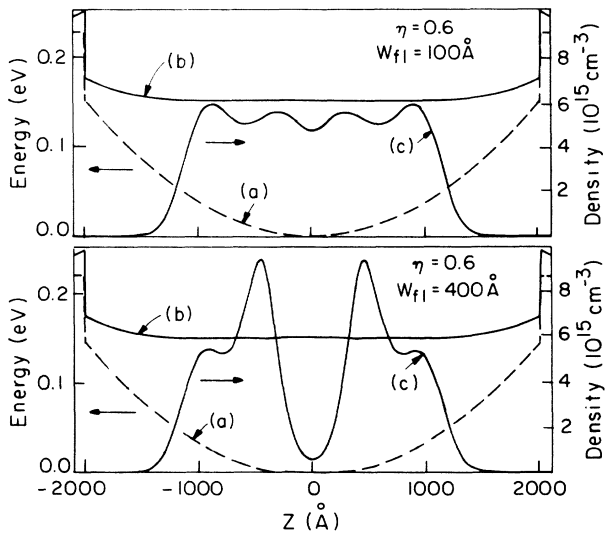

FIG. 7. Potential and charge density in a WPQW for two different widths of the region of flat potential $W_{\rm fl}=100$ and 400 Å. The fractional occupation is $\eta=0.6$. Curve (a) shows the bare potential $V(z)=V_1(z)+V_{\rm fl}(z)$ for the well, and curve (b) shows the total self-consistent potential $V_T(z)$. Curve (c) shows the self-consistent charge-density profile $n(z)$. The parameters of the WPQW are given in the text.

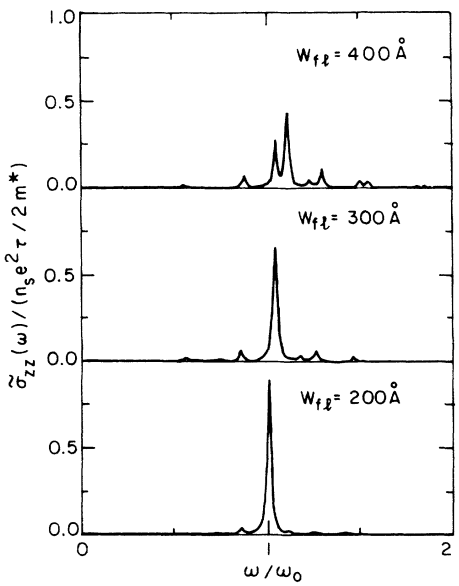

FIG. 8. Calculated real part of the dynamical conductivity $\tilde{\sigma}_{zz}(\omega)$ in a WPQW for different values of the width of the region of flat potential. The fractional occupation η is 0.6. The parameters of the WPQW are given in the text. The value of the phenomenological relaxation time, τ, is $0.01\omega_0$.

levels tend to become degenerate, as expected for two 2D electron gases. This is seen more clearly in Fig. 7, where the self-consistent charge-density profile is plotted for two values of W_{fl}. For $W_{fl}=400$ Å, the charge lies mostly to the sides of the barrier created by $V_{fl}(z)$.

As in the case of negative quartic term, the splitting of the charge-density profile strongly affects the optical-absorption spectrum, shown in Fig. 8. As W_{fl} increases, different peaks, with comparable intensities, appear around the frequency ω_0.

IV. SUMMARY

An electron gas in a perfect parabolic quantum well absorbs light only at the bare harmonic oscillator frequency.[12] In this work we have studied the changes that different perturbations induce on the ir optical-absorption spectrum of wide parabolic quantum wells. Three different types of effects have been considered: size effects, important when the well is overfilled; effects of a quartic term added to the confining potential; and effects of a region of flat potential in the center of the well. When the strength of any of these perturbations is small enough, the effect on the ir absorption spectrum is the same, namely (i) a shift of the main peak due to a shift in the frequency of oscillation of the center of mass of the electrons, and (ii) the appearance of new peaks around the main peak. The additional peaks had zero intensity in the ideal parabolic case, because they correspond to forbidden transitions. With the perturbations, the wave functions change and the transitions are no longer forbidden. The number of additional peaks and their positions depend on the particular form of the perturbation.

When the strength of the perturbation increases, the importance of the parabolic potential decreases, and the charge density in the electron slab becomes less and less uniform. When the uniformity is lost, several peaks with comparable intensities appear in the ir absorption spectrum.

Our LDA calculations are consistent with the result of Ref. 12, in that the optical-absorption spectrum we calculate in the absence of imperfections shows only one peak, which falls at precisely the expected frequency. On the other hand, one should not view this as strong confirmation that the LDA treats the electron-electron interaction accurately. The result of Ref. 12 holds for any interaction of the form $V(\mathbf{r}-\mathbf{r}')$, whether Coulombic or not. Our agreement with the general result shows only that, as we have used it, the LDA respects the translational invariance of the electron-electron interaction.

Also, the result of Ref. 12 implies that we must find an exact cancellation in our calculations of the depolarization term and the vertex-correction term by the corrections to the quasiparticle energy spacing due to the electron-electron interaction. In fact, we find that the cancellation also occurs when the vertex-correction term, Eq. (12), and the exchange-correlation potential, V_{xc}, are simultaneously omitted. This occurs because the depolarization term, Eq. (11), and the vertex-correction term separately cancel the effects of the Hartree and the exchange-correlation potentials, respectively.

ACKNOWLEDGMENTS

We thank P. F. Hopkins, R. Westervelt, A. C. Gossard, H. Ehrenreich, S. Das Sarma, and R. D. Meade for useful discussions. One of us (L.B.) wishes to acknowledge support from Spain's Ministerio de Educación y Ciencia. This work was supported by the U.S. National Science Foundation (NSF) through the Harvard University Materials Research Laboratory and Grant No. DMR-88-17291, by U.S. Defense Advanced Research Projects Agency (DARPA) through Office of Naval Research (ONR) Contract No. N00014-86-K-0033, and by St. John's College, Cambridge, England.

[1]D. Pines, *The Many-Body Problem* (Dunod-Willey, New York, 1959).

[2]A. C. Gossard, B. I. Halperin, and R. M. Westervelt (unpublished work); B. I. Halperin, Jpn. J. Appl. Phys. **26**, Suppl. 26-3, 1913 (1987).

[3]See, for example, K. Ploog, J. Cryst. Growth **81**, 304 (1987) and references therein.

[4]See, e.g., T. Ando, A. B. Fowler, and F. Stern, Rev. Mod. Phys. **54**, 437 (1982); *The Physics of the Two-Dimensional Electron Gas,* edited by J. T. Devreese and F. M. Peeters (Plenum, New York, 1987).

[5]We restrict ourselves to concentrations of aluminum lower than 0.44, at which value the X valley becomes the minimum of the conduction band. See, for example, F. Flores and C.

Tejedor, J. Phys. C **20**, 145 (1987).

[6]M. Sundaram, A. C. Gossard, J. H. English, and R. M. Westervelt, Superlatt. Microstruct. **4**, 683 (1988); E. G. Gwinn, R. M. Westervelt, P. F. Hopkins, A. J. Rimberg, M. Sundaram, and A. C. Gossard, Phys. Rev. B **39**, 6260 (1989); E. G. Gwinn, P. F. Hopkins, A. J. Rimberg, R. M. Westervelt, M. Sundaram, and A. C. Gossard, in *High Magnetic Fields in Semiconductors Physics II,* edited by G. Landwehr (Springer-Verlag, New York, 1989).

[7]M. Shayegan, T. Sajoto, M. Santos, and C. Silvestre, Appl. Phys. Lett. **53**, 791 (1988); T. Sajoto, J. Jo, L. Engel, M. Santos, and M. Shayegan, Phys. Rev. B **39**, 10464 (1989); M. Shayegan, T. Sajoto, J. Jo, M. Santos, and H. D. Drew, *ibid.* **40**, 3476 (1989).

[8]A. J. Rimberg and R. M. Westervelt, Phys. Rev. B **40**, 3970 (1989).

[9]M. P. Stopa and S. Das Sarma, Phys. Rev. B **40**, 10048 (1989).

[10]L. Brey and B. I. Halperin, in Proceedings of the Eighth International Conference on the Electronic Properties of Two-Dimensional Systems, Grenoble, France, 1989 [Surf. Sci. (to be published)]; Phys. Rev. B **40**, 11634 (1989).

[11]K. Karraï, H. D. Drew, M. W. Lee, and M. Shayegan, Phys. Rev. B **39**, 1426 (1989); K. Karraï, X. Ying, H. D. Drew, and M. Shayegan, *ibid.* **40**, 12020 (1989).

[12]L. Brey, N. F. Johnson, and B. I. Halperin, Phys. Rev. B **40**, 10647 (1989).

[13]P. Hohenberg and W. Kohn, Phys. Rev. **136**, B864 (1964); W. Kohn and L. J. Sham, *ibid.* **140**, A1133 (1965).

[14]See, e.g., R. O. Jones and O. Gunnarson, Rev. Mod. Phys. **61**, 689 (1989).

[15]L. J. Sham and W. Kohn, Phys. Rev. **145**, 561 (1966).

[16]F. Stern and S. Das Sarma, Phys. Rev. B **30**, 840 (1984).

[17]We use the exchange-correlation potential suggested by L. Hedin and B. I. Lundqvist, J. Phys. C **4**, 2064 (1971). Since we suppose a constant effective mass and dielectric constant across the well, this potential is continuous across the parabolic well. See the discussion in Ref. 16.

[18]W. B. Chen, Y. J. Chen, and E. Burstein, Surf. Sci. **58**, 263 (1976); S. J. Allen, D. C. Tsui, and B. Vinter, Solid State Commun. **20**, 425 (1976).

[19]T. Ando, Z. Phys. B **26**, 263 (1977).

[20]A. Tselis and J. J. Quinn, Surf. Sci. **113**, 362 (1982); K. S. Yi and J. J. Quinn, Phys. Rev. B **27**, 1184 (1983); **27**, 2396 (1983).

[21]D. A. Dahl and L. J. Sham, Phys. Rev. B **16**, 651 (1977).

[22]H. Ehrenreich and M. H. Cohen, Phys. Rev. **115**, 786 (1959); F. Stern, Phys. Rev. Lett. **18**, 546 (1967); E. D. Siggia and P. C. Kwok, Phys. Rev. B **2**, 1024 (1970).

[23]W. Kohn and L. J. Sham, Phys. Rev. **137**, A1697 (1965). N. D. Lang, in *Solid State Physics,* edited by H. Ehrenreich, F. Seitz, and D. Turnbull (Academic, New York, 1973), Vol. 28, p. 225.